Available online at www.CivileJournal.org

Civil Engineering Journal

(E-ISSN: 2476-3055; ISSN: 2676-6957)

Vol. 9, No. 10, October, 2023

Parametric Analysis of Horizontal Static and Dynamic Behavior in Different Types of Masonry Structures

Georgios Xekalakis [1*], Dimitris Pitilakis [2], Giulio Zuccaro [3], Petros Christou [1, 4]

[1] *Frederick Research Center, Pallouriotissa, Nicosia 1036, Cyprus.*

[2] *Department of Civil Engineering, Aristotle University of Thessaloniki, Thessaloniki 54636, Greece.*

[3] *University of Naples Federico II, PLINIVS-LUPT Study Centre, Napoli 80134, Italy.*

[4] *Frederick University of Cyprus, Pallouriotissa, Nicosia 1036, Cyprus.*

Received 07 June 2023; Revised 04 September 2023; Accepted 15 September 2023; Published 01 October 2023

Abstract

This article introduces the "Pre-seismic Survey Form for Masonry" (PRISM), a simplified tool for evaluating masonry structures. It aims to be user-friendly for both experienced surveyors and beginners. The primary objective is to develop PRISM as an efficient means of gathering relevant data that influences the diverse behaviors exhibited by masonry structures, covering both structural and non-structural aspects. PRISM's development involves a parametric method for identifying critical parameters by analyzing drift results from the response spectrum and horizontal static analyses. These analyses are performed on common masonry structures in European Mediterranean nations. The study investigates various factors, including facade openings, materials around openings, wall thickness, ground type, ground acceleration (g), and principal structural material. By examining 300 2D models created in SAP2000, correlations in structural responses are established. The findings of the parametric analysis significantly enrich the qualitative and quantitative comprehension of structural responses. This advancement contributes to the contemporary knowledge of prevalent masonry structures within European Mediterranean regions. The PRISM survey form employs a numeric rating scale format. Notably, PRISM enables surveyors to access field results, minimizing reliance on computers quickly. The form's design also ensures accessibility and data reliability, making it universally applicable while maintaining simplicity.

Keywords: Masonry Structures; Parametric Analysis; FE Modelling; Exposure; Risk Assessment; Resilience.

1. Introduction

Masonry structures have played a fundamental role in shaping the architectural landscape of Mediterranean European countries, representing an embodiment of cultural heritage and historical significance [1]. The preservation of historical masonry structures has triggered extensive discussions, particularly in the past fifty years, due to their unquestionable significance in social and economic aspects [2]. These structures, characterized by their unique construction techniques and the use of traditional building materials, have stood the test of time, withstanding numerous natural and anthropogenic hazards throughout the centuries. However, one prominent threat looms large over these structures: earthquakes. The Mediterranean region is known for its high seismic activity, often resulting from collisions between the Eurasian and African tectonic plates [3]. Consequently, masonry structures in this region face substantial vulnerability to seismic events, necessitating a comprehensive understanding of their seismic risk profiles. Without adequate risk assessment methodologies and strategic mitigation plans, these invaluable structures risk severe damage or complete loss in a significant earthquake [4].

* Corresponding author: res.xk@frederick.ac.cy

http://dx.doi.org/10.28991/CEJ-2023-09-10-015

Recognizing the urgency to safeguard the national heritage embodied within these masonry structures, it is imperative to develop innovative approaches that combine advanced seismic risk assessment techniques [5-7], geospatial technologies and artificial intelligence programming [8–10], and pre-seismic survey forms [11]. The synergy between these components can significantly contribute to creating exposure maps, enabling decision-makers and stakeholders to identify high-risk areas and prioritize retrofitting measures effectively [12, 13]. By adopting a proactive stance, Mediterranean European countries can minimize potential loss, enhance resilience, and preserve their invaluable cultural heritage for future generations.

This paper aims to introduce a simplified pre-seismic survey form for masonry structures, utilizing a parametric (numerical) analysis conducted with the assistance of SAP2000 software [14]. In this analysis, 2D models were developed and subjected to horizontal static and dynamic loading through response spectrum analyses, with variations in structural and non-structural components being tested.

This study aims to introduce a user-friendly pre-seismic survey form called PRISM (Pre-Seismic Survey Form for Masonry) for masonry structures. The goal is to use this tool to ensure minimal safety requirements are met to withstand earthquakes. It is anticipated that PRISM can be efficiently utilized by experienced surveyors, as well as students or junior engineers, to perform visual inspections and promote regular monitoring of buildings. In several countries, obtaining information on both structural and non-structural components of a building is challenging, as census data are often restricted for private use or the land survey department's functionality needs to be improved. The essential advantage of this survey form lies in its user-friendly and efficient completion process and scoring system, which enable quick retrieval of results.

2. Structural Materials

Load-bearing masonry structures hold significant historical significance in numerous Mediterranean countries. Despite these countries' varying sizes and economic strengths, including Cyprus, Malta, Greece, Portugal, Italy, and Spain, they all showcase a remarkable abundance of structures primarily constructed before the 1960s using load-bearing masonry techniques. The choice of structural materials in these regions varied based on the local environment and prevailing weather conditions, contributing to the distinctive character of each place. In warmer and drier climates, constructions crafted from adobe and tufa [15] are commonly found, whereas stone structures become more prevalent as we move further north. Factory-produced materials such as concrete blocks and clay bricks have emerged in recent years. Around 2000, a novel material, Aerated Concrete Masonry [16], or Alpha Block, appeared.

Adobe stands out as one of the most sustainable building materials, composed of locally abundant earth-based resources. However, its handmade nature makes it the most "unpredictable" material, as the mixture ratios and ingredients can vary even in neighboring areas. Stone masonry is environmentally friendly, typically sourced from nearby regions or rivers. Stones were stacked on each other, with or without a binding mixture, known as dry-stone wall construction. Constructions of adobe or stone are traditionally more massive than today's buildings, and their behavior during an earthquake is difficult to define. Tufa played a central role in the traditional architecture of many southern Mediterranean regions. These stones were minimally processed to ensure better fitting. Certain buildings, particularly public structures, exhibit a higher level of stone processing. However, generally, walls were predominantly constructed with partially or entirely uncarved stones. Carved stones were only employed at corners and openings to reinforce the weakest sections of the structure. It is essential to highlight that these structures, lacking seismic considerations, represent the most vulnerable aspect of load-bearing masonry construction.

New regulations, such as EC6, consider more modern materials like concrete blocks, clay bricks, and alpha blocks. These materials have gained recognition and are considered in the context of building codes and regulations. EC6 (Eurocode 6) specifically addresses the design of masonry structures and provides guidelines for using various masonry materials, including concrete blocks, clay bricks, and other contemporary products like alpha blocks.

Each primary construction material exhibits distinct mechanical properties (Table 1) and construction methods. The referenced values shown in Table 1 have been derived from existing literature sources [17–20].

Table 1. Mechanical characteristics of the structural materials

	Adobe	Aerated Concrete	Clay bricks	Concrete blocks	Stone	Tufa
Density (kg/m^3), d	1300	500	1890	2345.35	2360	1270
Modulus of Elasticity (kN/m^2), E	18000	1500000	5170000	2550000	2080000	5070000
Poisson ratio, ν	0.30	0.2	0.2	0.19	0.2	0.28
Shear Modulus (kNm^{-2}), G	6923	625000	2154167	1071429	866667	1980468.80

In the case of residential buildings, the thickness of the external masonry varies depending on the chosen material. For instance, load-bearing masonry constructed with adobe, tufa, or stone typically had a minimum thickness of 40 cm, but it could reach up to 80 cm. On the other hand, walls composed of materials like concrete blocks, clay bricks, and alpha blocks had a thickness ranging from 20 to 25 cm.

These structures encountered a significant challenge due to inadequate connectivity between the intersected walls and accumulated stresses within the primary masonry structure. Even without seismic regulations, it was evident that adobe and tufa constructions were highly susceptible to earthquakes. To address this issue, one technique employed involved the insertion of timber (wooden) ring beams (TRB) along the height of the wall, typically positioned at 0.8-1.2 m intervals [6]. Cypress was commonly utilized for these beams due to its specific material properties. The Young's modulus (E) of the cypress was measured to be approximately 10.98GPa, Poisson's ratio (ν) of 0.18, and the density of the cypress was determined to be 500 kg/m³. This approach aimed to stabilize the structure and minimize displacement during seismic events.

After an on-site investigation in a region of Cyprus for the ISTOS [21] project purposes, it was observed that the openings of the load-bearing masonry structures are at most 30% of the total surface area of each face. This observation mainly concerns residential buildings, most of which were made of adobe and, to a lesser extent, stone and tufa, which follow the same pattern. It was also noted that the primary material of the opening frames (Table 2) was wood and aluminum, with some exceptions where PVC and fiberglass were used [22-25].

Table 2. Mechanical properties of the opening's frame materials

	Aluminum	**Fiber-glass**	**PVC**	**Wood**
Density (kg/m^3), d	2710	1850	480	2490
Modulus of Elasticity (kN/m^2), E	69000000	2800000	9200000	86000000
Poisson ratio, *v*	0.33	0.32	0.47	0.22
Shear Modulus (kN/m^2), G	25939850	1060606.10	3129251.70	35245902

3. Methodology

The methodology comprises various steps described below. To commence, a pivotal undertaking involved defining, based on a thorough literature review, the primary masonry typologies prevalent in Mediterranean countries. This encompassed identifying the critical structural and non-structural components that influence structural behavior and delineating the mechanical properties of principal construction materials. The process entailed crafting 2D Finite Element models within the SAP2000 software. Two types of analyses were executed with a focus on interstorey drift as a pivotal metric. The first centered around a static analysis, wherein factors such as façade openings, the corresponding framing around these openings, and the role of timber ring beams within adobe masonry structures were taken into meticulous account. The second encompassed a dynamic analysis, leveraging response spectrum techniques. This facet also incorporated considerations of ground type and ground acceleration. These facets collectively yielded various results, consistently anchored by the interstorey drift metric. The decision was made to standardize the values against the "immediate Occupancy" damage limit state, specifically designed for load-bearing masonry structures to enable meaningful comparisons. Employing this normalization procedure, a set of scoring system tables was derived. These tables encompassed the initial scoring values associated with a structure, predicated on the underlying ground acceleration and ground type.

Moreover, they encompassed a reduction factor applicable to adobe structures fortified with timber ring beams. The tables also incorporated correction factors contingent upon the extension of façade openings and multiplication factors to account for diverse framing materials around openings, some of which contribute to resisting horizontal loads. The overarching goal of this endeavor was to produce a streamlined survey form tailored for masonry structures. This tool empowers surveyors to promptly gauge the vulnerability status of the structure under assessment, thereby encapsulating the extensive insights gleaned from this comprehensive methodology. The entire process outlined above is visually represented in the accompanying flowchart provided in Figure 1 below.

The current state of practice favors employing macro-modeling as the preferred approach to advance the development of the models. In order to implement the parametric analysis, 300 2D finite element models were created in SAP2000. The dimensions of the façade were defined as 3m in height and 6m in length. The masonry walls were simulated as a homogeneous and isotropic continuum material [26] using shell elements implementing the Mindlin/ Reissner formulation [27], which accounts for the shear deformations in the elements. A 10cm x 10cm grid mesh has been implemented to achieve optimal results. To ensure balanced displacement on both sides, a diaphragmatic constraint has been applied to the upper section of the wall.

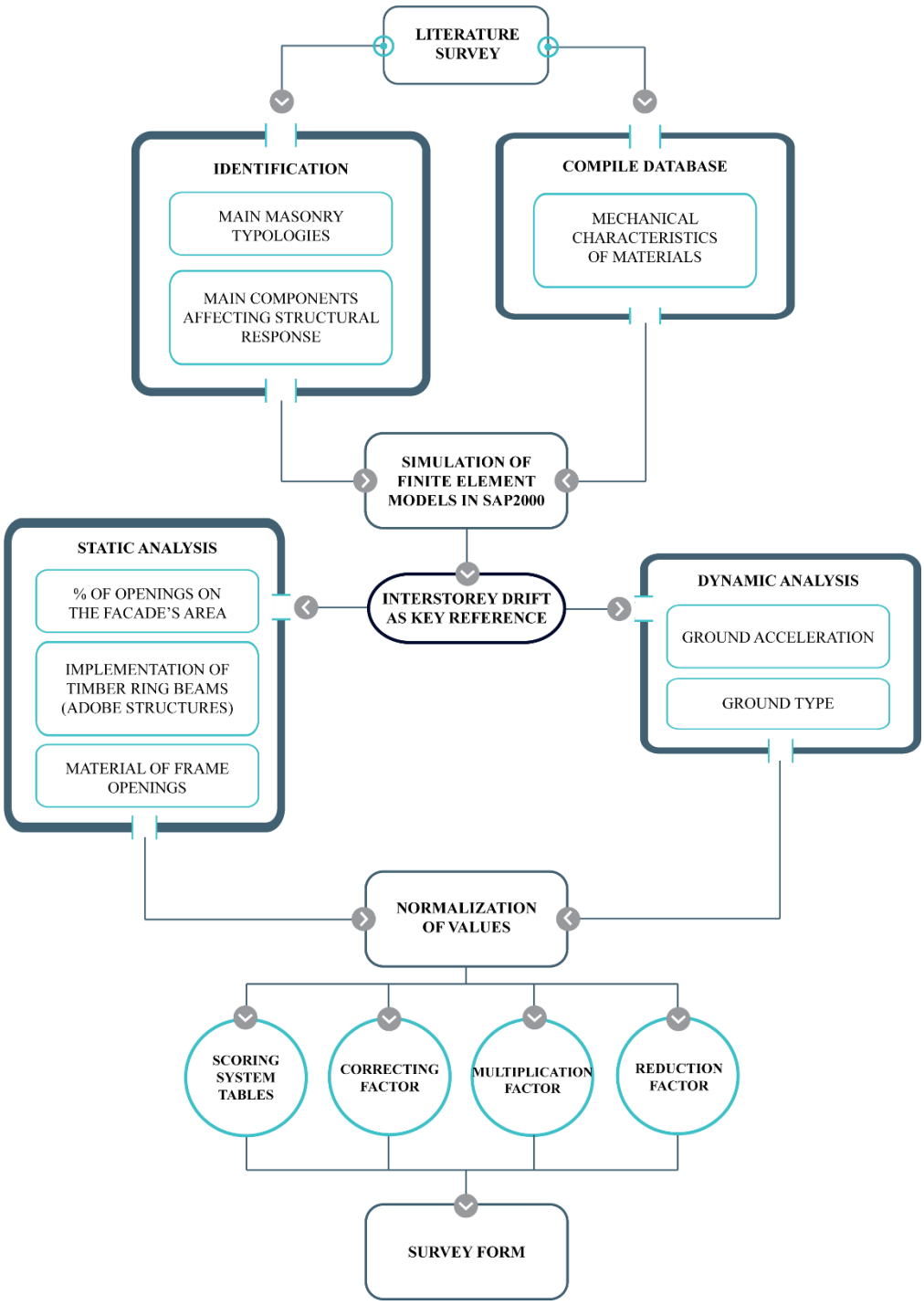

Figure 1. Integrated Methodology Flowchart for Assessing Mediterranean Masonry Structure Vulnerability

Load-bearing masonry structures must be designed and planned to effectively distribute vertical and dynamic forces across the entire masonry area. The size of openings on each face should be reasonably limited to ensure optimal resistance to seismic loads. During the on-site inspection, it was evident that these openings typically did not exceed 25-30% of the face's total surface area.

Considering the above, the initial stage consisted of 6 different models (Figure 2), representing the façade of a house made of load-bearing masonry, which were separated according to the percentage of openings (Table 3) covering the total surface of the façade. The primary objective was to quantitatively assess how the stiffness is affected by different opening sizes in the face. By doing so, we could gain valuable insights into the structural behavior and the degree of stiffness reduction associated with varying opening sizes. The models mentioned above were combined with the 6 + 1 (adobe with timber ring beams) main structural materials considered in this research and characterized by different mechanical characteristics. The purpose of this first test was to extract a first estimate of the extent to which the width of the openings reduces the stiffness of the structure based on the displacement (Table 4) after the application of a static load of 20kN and also to create a table with the percentage reduction of stiffness (Table 5). The typical wall thickness encountered in each of the above cases was considered during the analysis.

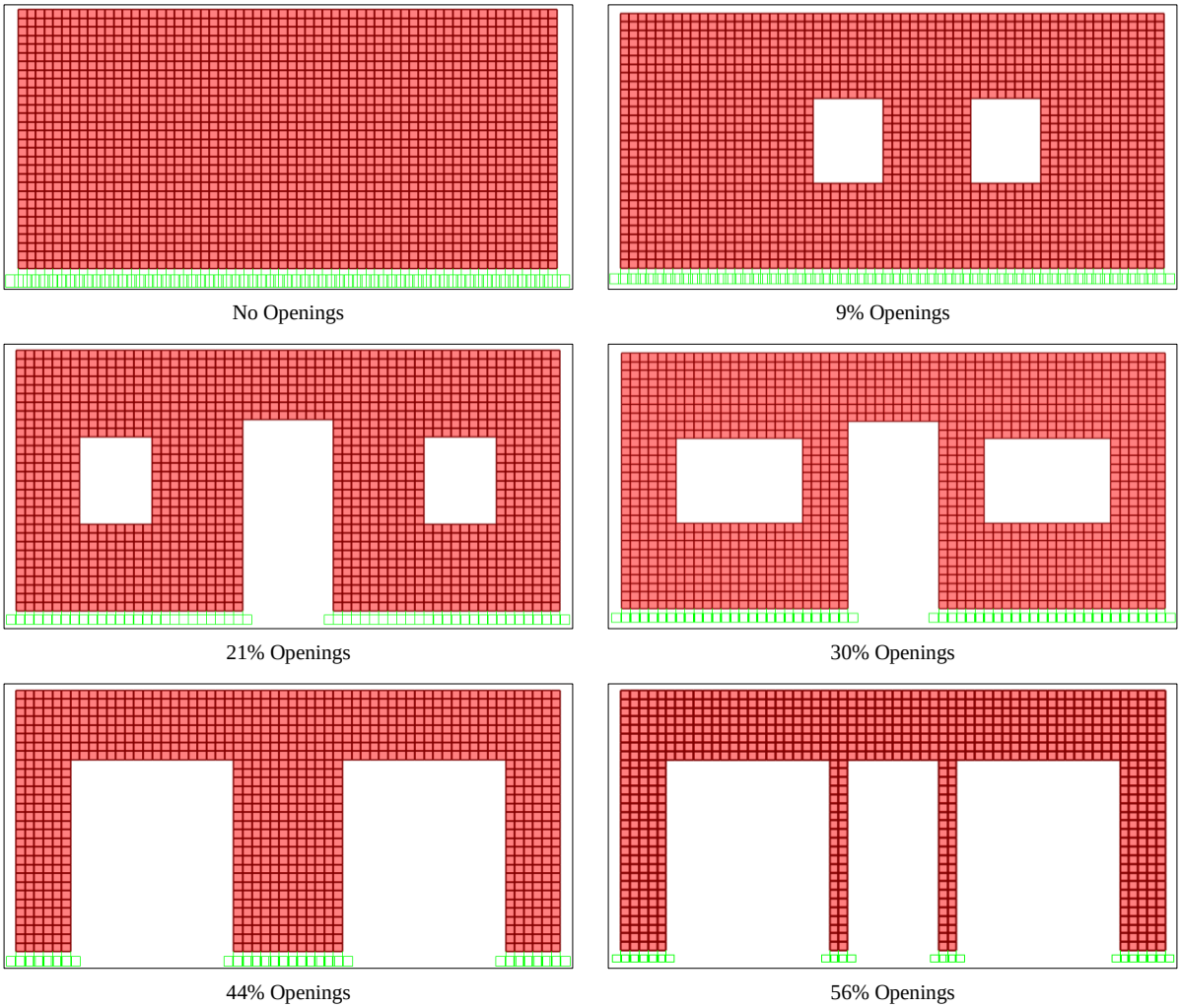

Figure 2. Façade's view

Table 3. Extension and dimension of façade's openings

Opening's range	No.	Door's dimensions (m)	No.	Window's dimensions (m)	Total extend (%)
<10%	-	-	2	0.8 × 1	9
10% - 25%	1	1 × 2.2	2	0.8 × 1	21
25% - 30%	1	1 × 2.2	2	1.4 × 1	30
30% - 50%	-	-	2	1.8 × 2.2	44
>50%	1	1 × 2.2	2	1.8 × 2.2	56

Table 4. Displacement (m) of the single storey 2D model after the lateral static load analysis

Material	% Openings					
	0%	9%	21%	30%	44%	56%
Adobe	0.005	0.008	0.011	0.018	0.036	0.15
Adobe with TRB	0.005	0.0067	0.009	0.012	0.028	0.12
Alpha blocks (thickness 20cm)	0.0001	0.0002	0.0003	0.0004	0.0007	0.0035
Clay brick (thickness 20cm)	3.44E-05	5.43E-05	7.6E-05	0.0001	0.0002	0.001
Concrete blocks (thickness 20cm)	1.36E-05	2.04E-05	2.9E-05	4.6E-05	9.2E-05	0.0004
Stone	4.27E-05	6.7E-05	9.4E-05	0.0002	0.0003	0.0013
Tufa	1.83E-05	2.78E-05	4E-05	6.3E-05	0.0001	0.0005

Table 5. Percentage decrease of wall's stiffness based on the opening's surface

Material	% Openings					
	0%	< 10%	10%-25%	25%-30%	30%-50%	>50%
Adobe	0.00	-0.01	-0.01	-0.03	-0.06	-0.29
Adobe with TRB	0.00	0.00	-0.01	-0.01	-0.05	-0.23
Alpha blocks (thickness 20cm)	0.00	-0.01	-0.02	-0.03	-0.06	-0.34
Clay brick (thickness 20cm)	0.00	-0.01	-0.01	-0.02	-0.05	-0.28
Concrete blocks (thickness 20cm)	0.00	-0.01	-0.01	-0.02	-0.06	-0.28
Stone	0.00	-0.01	-0.01	-0.04	-0.06	-0.29
Tufa	0.00	-0.01	-0.01	-0.02	-0.04	-0.26

The subsequent phase examined how the openings' structural framework influences the wall's lateral response and, consequently, its resistance against horizontal forces. As previously mentioned, a recent survey of buildings in one municipality in Nicosia (Cyprus) revealed that most load-bearing masonry structures feature a façade with openings occupying approximately 25–30% of the total surface area. Thus, it was decided that the upcoming analysis would focus on models incorporating these particular percentages. As stated in Section 2, the window frames were observed to be constructed using four different materials: wood, aluminum, PVC, and fiberglass. These elements surrounding the wall openings were modeled using frame elements. The frame section was developed using the Section Designer feature of the SAP2000 software, with dimensions of 5cm × 5cm. To assess the impact of the frames, a static horizontal load of 20 kN was applied after installing the windows in the wall openings. The goal was to observe the contribution, if any, of each material against the horizontal displacement. The analysis results are summarized in Table 6, which presents the initial displacement without the frame elements around the openings, the displacement with the frame implementation, and the percentage of contribution from the frames in each case.

Table 6. Contribution of different frame types against horizontal displacement (m)

Structural material	Opening's Frame Material					
	Aluminum			Fiberglass		
	With	Without	Contribution (%)	With	Without	Contribution (%)
Adobe	0.0074	0.018	59	0.0071	0.018	60
Alpha block	0.0003	0.0004	25	0.0003	0.0004	25
Clay brick	9.6E-05	0.0001	4	9.3E-05	0.0001	7
Concrete block	4.1E-05	4.6E-05	11	4E-05	4.6E-05	13
Dry-stone	0.00012	0.0002	44	0.00014	0.0002	43
Tufa	5.4E-05	6.3E-05	14	5.3E-05	6.3E-05	16
Structural material	**Opening's Frame Material**					
	PVC			**Wood**		
	With	**Without**	**Contribution (%)**	**With**	**Without**	**Contribution (%)**
Adobe	0.011	0.018	39	0.009	0.018	50
Alpha block	0.0004	0.0004	0	0.0004	0.0004	0
Clay brick	0.0001	0.0001	0	0.0001	0.0001	0
Concrete block	4.6E-05	4.6E-05	0	4.6E-05	4.6E-05	0
Dry-stone	0.00015	0.0002	25	0.00014	0.0002	30
Tufa	6.2E-05	6.3E-05	1.6	6.1E-05	6.3E-05	3

Additionally, 2D models were generated for two-roof buildings to study their behavior accordingly. However, in this scenario, the displacement of the upper slab was not recorded. Instead, the inter-story drift, as defined by EC8 (Eurocode 8), was measured. Table 7 presents the interstorey drift values in meters for each type of masonry, categorized by the main structural material and the width of the openings. Notably, materials with a low Young's modulus, like adobe and alpha block, exhibit significantly larger interstorey drifts than other materials, particularly when the width of the openings exceeds 50%. Table 8 presents a normalization of the values based on the model without openings. The purpose is to analyze and deduce the reduction in stiffness for the models with larger openings, expressed as one less coefficient unit in percentage. This allows us to observe the relationship between the stiffness reduction and the size of the openings more effectively.

Table 7. Displacement (m) of the 2D 2storey model after the lateral static load analysis

Material	% Openings					
	0%	9%	21%	30%	44%	56%
Adobe	0.017	0.025	0.03	0.045	0.09	0.35
Adobe with TRB	0.0005	0.0009	0.0012	0.0017	0.0027	0.011
Alpha blocks (thickness 20 cm)	0.02	0.04	0.05	0.07	0.14	0.45
Clay brick (thickness 20 cm)	1.36E-04	0.00025	0.00025	0.00043	0.0009	0.0021
Concrete blocks (thickness 20 cm)	5.64E-05	0.0001	0.0001	0.0002	0.0004	0.0011
Stone	1.5E-04	0.0003	0.0004	0.0005	0.001	0.0031
Tufa	7.67E-05	0.0001	0.0002	0.0002	0.0005	0.0016

Table 8. Percentage reduction of the stiffness of the walls based on the opening's surface

Material	% Openings					
	0%	< 10%	10%-25%	25%-30%	30%-50%	>50%
Adobe	0.00	0.00	-0.01	-0.02	-0.04	-0.20
Adobe with TRB	0.00	-0.01	-0.01	-0.02	-0.04	-0.21
Alpha blocks (thickness 20 cm)	0.00	-0.01	-0.02	-0.03	-0.06	-0.22
Clay brick (thickness 20 cm)	0.00	-0.02	-0.02	-0.03	-0.06	-0.15
Concrete blocks (thickness 20 cm)	0.00	-0.01	-0.01	-0.03	-0.06	-0.19
Stone	0.00	-0.02	-0.03	-0.03	-0.07	-0.21
Tufa	0.00	0.00	-0.02	-0.02	-0.06	-0.20

4. Parametric Analysis

When a building is examined, its location is vital in addition to the structural and non-structural components. This implies that characteristics such as the ground type and the main seismic acceleration defined for the region concerned by the seismic maps [28] or the EC8 NATIONAL ANNEXES [29] for the European countries should be considered.

Knowing the above and aiming at implementing a survey form with a scoring system, a response spectrum analysis was conducted for the five ground categories mentioned in EC8 with an acceleration of 0.1-0.5g. The q based on the literature for load-bearing unreinforced masonry buildings was equal to 1.5 [30]. For further analysis, 300 models were created since six structural materials for single and double-storey buildings had to be considered in addition to the ground type categories and accelerations.

During an earthquake, wall failure usually occurs in the out-of-plane (OOP) direction before the walls attain their in-plane (IP) strength. However, the available literature on OOP analyses for masonry structures still needs to be expanded, making obtaining the corresponding damage limit state values challenging. Although previous studies have conducted numerical investigations specifically focusing on stone [31] and clay brick walls [32], they fail to cover the range of the structural materials considered in this research, such as adobe bricks and tufa. Considering this, we have decided to proceed with analyzing the in-plane response of the masonry wall while also considering the corresponding damage limit states.

After the results of the response spectrum analyses were explained and recorded, the numerical limit for the vulnerability classification of the buildings had to be decided. Concerning the damage limit states, they are typically categorized into four main categories, namely Immediate Occupancy (IO), Life Safety (LS), Collapse Prevention (CP), and Collapse (C). Based on the research explained by Zavala et al., 2019 [33], the damage limit states for load-bearing masonry structures whose handmade components have been chosen (Table 9). Between the handmade limits and the industrial-made counterparts, the first ones were selected to be in the margin of safety.

Table 9. Drift values (m)

IO	LS	CP	C
0.0004	0.0013	0.0029	0.0033

The numbers above have been normalized based on the limit of the IO value having, as a result, the following Table 9. Table 10 shows the normalized values based on the "Immediate Occupancy" corresponding value.

Table 10. Normalized drift values

IO	LS	CP	C
1	3.25	7.25	8.25

As mentioned earlier, PRISM relies on a scoring system to evaluate and measure different aspects of a building's condition, performance, or adherence to specific standards. Scoring systems, such as the one used in FEMA survey forms, are widely employed for this purpose. The numeric rating scale is the most commonly utilized scoring system in building surveys. It involves assigning numerical values to various building components based on predefined criteria. For instance, a rating scale ranging from low to high numbers may be employed to assess the condition of different building elements. In our case, higher scores indicate a more vulnerable structure.

The results of the response spectrum analyses have been normalized with the same number for consistency (0.0004) and are shown below (Table 11). The number of each cell corresponds to a ground type, ground acceleration, and different structural materials. These numbers work as the survey's starting values form the scoring system and are unitless.

Table 11. Starting values of the case studies

ag/g	Adobe (single storey)					Adobe (two storeys)				
	Ground type					Ground type				
	A	B	C	D	E	A	B	C	D	E
0.1	1	1.25	1.25	1.5	1.5	1.25	2.5	2.75	3.5	2.75
0.2	2	2.5	2.5	3	3	3	3.75	4.5	5.25	4.5
0.3	3	3.75	3.75	4.5	4.5	4	4.25	5.75	7	5.75
0.4	4	5	5	6	6	5.75	6.25	7.5	8.25	7.5
0.5	5	6.25	6.25	7.5	7.5	7.75	12.5	15	17.5	15
ag/g	**Alpha block (single storey)**					**Alpha block (two storeys)**				
0.1	0.00	0.00	0.00	0.00	0.00	0.01	0.01	0.01	0.01	0.01
0.2	0.01	0.01	0.01	0.01	0.01	0.02	0.02	0.02	0.03	0.03
0.3	0.01	0.01	0.01	0.01	0.01	0.03	0.04	0.04	0.04	0.05
0.4	0.01	0.01	0.01	0.02	0.02	0.03	0.04	0.04	0.05	0.05
0.5	0.02	0.02	0.02	0.02	0.02	0.04	0.05	0.05	0.05	0.06
ag/g	**Clay bricks (single storey)**					**Clay bricks (two storeys)**				
0.1	0.003	0.004	0.004	0.004	0.005	0.0035	0.005	0.004	0.005	0.005
0.2	0.006	0.008	0.004	0.008	0.008	0.0075	0.01	0.0075	0.01	0.01
0.3	0.009	0.011	0.005	0.013	0.013	0.01	0.0125	0.0125	0.015	0.015
0.4	0.013	0.015	0.013	0.016	0.018	0.015	0.015	0.015	0.0175	0.0175
0.5	0.018	0.019	0.018	0.020	0.021	0.02	0.02	0.0225	0.025	0.025
ag/g	**Stone (single storey)**					**Stone (two storeys)**				
0.1	0.01	0.01	0.01	0.02	0.02	0.03	0.03	0.03	0.03	0.04
0.2	0.02	0.03	0.03	0.02	0.03	0.05	0.06	0.06	0.06	0.08
0.3	0.03	0.04	0.04	0.04	0.04	0.08	0.08	0.08	0.09	0.10
0.4	0.04	0.05	0.05	0.04	0.05	0.11	0.13	0.13	0.13	0.20
0.5	0.06	0.06	0.06	0.05	0.08	0.13	0.13	0.13	0.13	0.30
ag/g	**Concrete block (single storey)**					**Concrete block (two storeys)**				
0.1	0.001	0.002	0.002	0.002	0.002	0.0035	0.005	0.004	0.005	0.005
0.2	0.003	0.003	0.003	0.004	0.004	0.0075	0.01	0.0075	0.01	0.01
0.3	0.004	0.005	0.005	0.005	0.005	0.01	0.0125	0.0125	0.015	0.015
0.4	0.005	0.006	0.006	0.007	0.007	0.015	0.015	0.015	0.0175	0.0175
0.5	0.006	0.008	0.008	0.009	0.009	0.02	0.02	0.0225	0.025	0.025
ag/g	**Tufa (single storey)**					**Tufa (two storeys)**				
0.1	0.002	0.0025	0.003	0.0028	0.003	0.005	0.0075	0.0065	0.0075	0.01
0.2	0.0043	0.005	0.005	0.0055	0.006	0.01	0.01	0.0125	0.01	0.015
0.3	0.0065	0.0075	0.008	0.0083	0.009	0.0175	0.0175	0.0175	0.0175	0.0225
0.4	0.0088	0.01	0.01	0.011	0.012	0.0275	0.03	0.0275	0.03	0.0325
0.5	0.011	0.0125	0.013	0.0138	0.015	0.035	0.0375	0.035	0.0375	0.0425

The values in Table 11 correspond to the outcomes obtained from masonry models with an opening percentage ranging from 25% to 30%. However, if the percentage of the opening deviates from this range, it becomes necessary to account for the correction factor indicated in Table 12. The column representing 25%-30% values contain zeros because, as stated, all initial values are calculated using this percentage. Subsequently, the remaining values are normalized to these initial values.

Table 12. Correcting factor based on the façade's openings

Structural material	Façade's Openings percentage					
	0%	< 10%	10%-25%	25%-30%	30%-50%	>50%
Adobe	-0.71	-0.43	-0.29	0.00	1.00	5.43
Alpha blocks	-0.71	-0.47	-0.29	0.00	0.59	5.47
Clay brick	-0.73	-0.50	-0.50	0.00	1.00	4.50
Concrete blocks	-0.72	-0.50	-0.50	0.00	1.00	4.50
Stone	-0.87	-0.40	-0.20	0.00	1.00	5.20
Tufa	-0.62	-0.50	0.00	0.00	1.50	7.00

In the specific scenario of an adobe structure subjected to a case study involving the incorporation of timber ring beams, an adjustment must be made to the initial value. This adjustment is based on the relationship between adobe masonry with and without ring beams, as depicted in Table 5. For this particular case, the reduction factors are provided in Table 13.

Table 13. Reduction factor for the adobe structures with TRB

	0	< 10%	10%-25%	25%-30%	30%-50%	>50%
Contribution of TRB	-0.03	-0.17	-0.23	-0.29	-0.57	-1.14

As stated in the "materials" section, the window frames play a significant role in the overall in-plane response of the structure. Table 6 illustrates the distinct contributions of each material. To obtain the final rating number, it is essential to multiply the current number by the abovementioned procedure associated with the specific case being examined. The coefficients in the table (Table 14) represent the remaining percentage after factoring in the frame's influence on the horizontal response.

Table 14. Opening's frame material multiplication factor

	Aluminum	Fiberglass	PVC	Wood
Adobe	0.41	0.4	0.61	0.5
Alpha block	0.75	0.75	1	1
Clay brick	0.96	0.87	1	0.93
Concrete block	0.89	0.87	1	0.98
Stone	0.56	0.57	0.75	0.7
Tufa	0.86	0.84	0.984	0.97

5. PRISM Survey Form

The simplified pre-seismic survey form, PRISM (Figure 3), for masonry structures can be exploited by both experienced surveyors and novice practitioners. PRISM is based on the ISTOS form and is divided into six sections. The first two sections refer to the survey information and building identification. In section 3, the user must fill in the boxes of the masonry construction material and the number of floors. Section 4 is referent only to the structures built with adobe blocks. Section 5 includes the percentage of openings on the building's façade and defines the material of the frame around the openings. Section 6 is about the geotechnical characteristics of the field. In the absence of such data, the information can also be drawn by the National Annex of Eurocode.

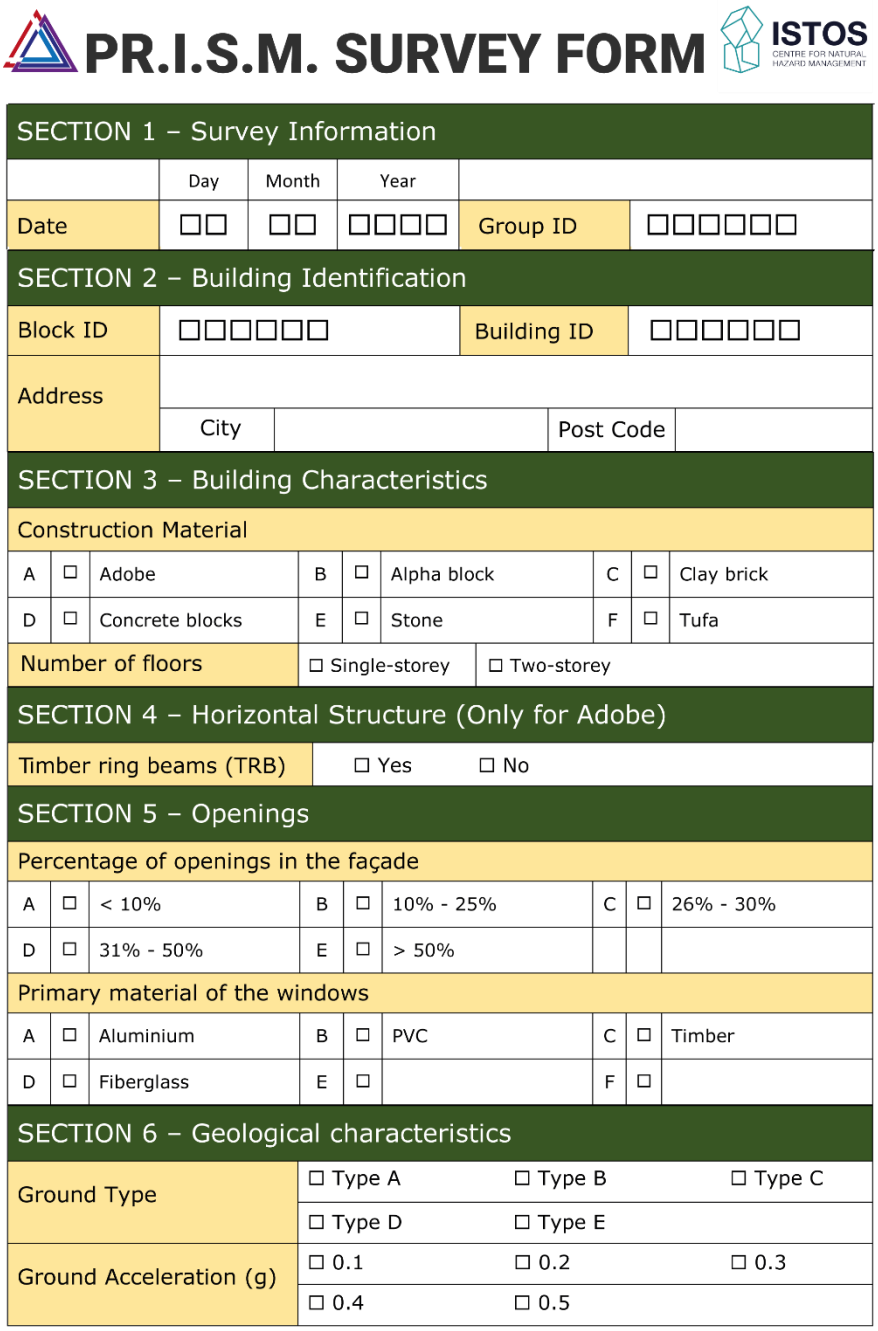

PR.I.S.M. SURVEY FORM ISTOS CENTRE FOR NATURAL HAZARD MANAGEMENT

SECTION 1 – Survey Information					
	Day	Month	Year		
Date	☐☐	☐☐	☐☐☐☐	Group ID	☐☐☐☐☐☐

SECTION 2 – Building Identification			
Block ID	☐☐☐☐☐☐	Building ID	☐☐☐☐☐☐
Address			
City		Post Code	

SECTION 3 – Building Characteristics								
Construction Material								
A	☐	Adobe	B	☐	Alpha block	C	☐	Clay brick
D	☐	Concrete blocks	E	☐	Stone	F	☐	Tufa
Number of floors	☐ Single-storey		☐ Two-storey					

SECTION 4 – Horizontal Structure (Only for Adobe)		
Timber ring beams (TRB)	☐ Yes	☐ No

SECTION 5 – Openings								
Percentage of openings in the façade								
A	☐	< 10%	B	☐	10% - 25%	C	☐	26% - 30%
D	☐	31% - 50%	E	☐	> 50%			
Primary material of the windows								
A	☐	Aluminium	B	☐	PVC	C	☐	Timber
D	☐	Fiberglass	E	☐		F	☐	

SECTION 6 – Geological characteristics			
Ground Type	☐ Type A	☐ Type B	☐ Type C
	☐ Type D	☐ Type E	
Ground Acceleration (g)	☐ 0.1	☐ 0.2	☐ 0.3
	☐ 0.4	☐ 0.5	

Figure 3. PRISM survey form

6. Discussion

The present research incorporates a parametric analysis to develop a pre-seismic survey form based on a scoring system exclusively for masonry structures. To conduct the analysis, 300 two-dimensional numerical models were generated using SAP2000. These models exhibited structural variations, encompassing different combinations of structural materials, varying percentages of openings on the façade, and distinct materials for the frames around the openings. Additionally, factors such as ground type and ground acceleration were considered.

To initiate the analysis, it was necessary to select a reference model. A recent on-site inspection of a Nicosia, Cyprus community revealed that most masonry structures were single-story buildings with façades comprising 25 - 30% openings. Based on these findings, the majority of the scoring values were derived. At the outset, six different models were utilized (depicted in Figure 2) to portray a wall constructed with load-bearing masonry. These models were categorized based on the proportion of openings (as outlined in Table 3) that adorned the entire façade area. The primary objective was to meticulously assess the impact of diverse opening dimensions on structural rigidity. Through this analysis, insightful information was aimed to be extracted about the architectural response and the extent of stiffness degradation linked to different opening magnitudes.

In the "Structural Materials" section, Table 1 presents the mechanical properties of the six analyzed structural materials. Notably, by examining the values of Young's modulus, one can quickly discern that adobe is the weakest material, thus indicating larger displacement values can be expected. This assumption is corroborated in Table 4, where the displacement values are displayed after implementing the horizontal static analysis. It is important to mention that the thickness of each wall corresponds to the actual design thickness based on the specific structural material. Each model was categorized into six groups (0%, <10%, 10%–25%, 26%–30%, 31%–50%, >50%) based on the percentage of openings on the façade. Table 4 presents the maximal displacement at the highest point after applying a static horizontal load of 20 kN to the model, correlated with the respective material properties. In seismic events, load-bearing masonry structures collectively withstand the dynamic horizontal forces, functioning as integral units. This contrasts with reinforced concrete structures, where the primary load resistance comes from columns and walls. In light of this distinction and guided by the stiffness formula for masonry ($K = AEI/h^3$, where I represents the moment of inertia) [34], we anticipate observing an amplified roof displacement as the effective length of contributing masonry diminishes against horizontal loading, as detailed in Table 4. Table 5 demonstrates the conversion of displacement into percentages, facilitating rapid assessment of the reduction in load-bearing masonry stiffness in relation to the expansion of openings in the simulation. This has been accomplished by normalizing the values relative to the displacement in scenarios where the façade lacks any openings. Instances where openings cover less than half of the façade exhibit stiffness reduction rates of up to 6%. Notably, a significant decrease in stiffness, ranging from 23% to 34%, occurs when opening coverage surpasses 50% of the façade. It is worth acknowledging that identifying such structures in reality proves challenging. Nevertheless, this examination was a comprehensive aspect of the study's scope.

Following a relevant literature review, it was noted that survey forms and similar research works [35] assess the condition of window frames in various openings, categorizing them as poor, mediocre, etc. Building upon this premise, extending this assessment to encompass the materials used in constructing these casings was deemed essential. This extension aimed to determine whether the chosen materials influenced the structural rigidity against horizontal forces. Table 6 illustrates the displacements experienced by each component before and after the introduction of frames to the openings. Upon examination of the data, it becomes evident that the incremental contribution is generally modest across most cases. However, noteworthy exceptions arise in adobe and dry-stone structures, where contributions can reach as high as 60%.

The subsequent step involved the incorporation of frames around the openings (casings). These frames were modeled as frame elements in SAP2000, utilizing a cross-section of 5cm x 5cm. Four different casing materials were tested for the openings. The lateral static load analysis results revealed significant contributions from aluminum and fiberglass frames in some instances, such as adobe and alpha block structures. At the same time, their impact was minimal in the remaining scenarios. Conversely, when the frame material was specified as wood or PVC, the contribution was nearly negligible, except in the case of adobe structures. This can be attributed to the mass and subsequent inertia of the walls; therefore, weaker frame materials like wood and PVC do not significantly influence the in-plane response of the wall.

As mentioned earlier, the analysis has incorporated both topographic and seismic characteristics. The relationship between the average shear wave velocity in the top 30 m ($V_{s,30}$) from the surface and displacements on the superstructure is evident from the data presented in Table 11, whereby smaller $V_{s,30}$ values result in larger displacements. An important aspect of vulnerability analysis is the intensity of dynamic events that typically occur in a region or country. Seismic maps of Europe indicate ground acceleration values between 0.1g and 0.5g in the areas surrounding the Mediterranean Sea. These values were tested using SAP2000 software to generate response spectrums, combining ground types and ground acceleration values to determine the maximum displacements for each structural type.

The response spectrum analyses were considered linear since most of the materials under consideration exhibit brittle behavior and possess stress-strain curves characterized by a minimal plastic region. However, specific damage limit states are required to define the fragility of the structures. These values were obtained from the existing literature and are presented in Table 9. It should be noted that this survey is based on a scoring system, which typically lacks units. To address this, all displacement values were first normalized by the Immediate Occupancy (IO) value provided in Table 9, resulting in the initial scoring values presented in Table 11. The correction factors presented in Table 12 were normalized based on the values obtained from models with 25-30% openings, along with the multiplication factors derived from the contribution of opening frames to the overall structure.

Considering the Vulnerability table of EMS98 [36], it was decided to create a corresponding table that represents the fragility of structures based on the numerical analyses conducted in this research. Certain assumptions needed to be made to achieve this, and a reference model was selected. In similar cases, median values are commonly used, particularly for ground type and ground acceleration. Consequently, the values corresponding to ground type C and ground acceleration of 0.3g were chosen as the reference point for creating the subsequent figure (Figure 4).

The primary categorization (principal taxonomy) of structures (represented by circles) in Figure 4 has been determined based on the scoring values, explicitly focusing on the values associated with single-storey structures with 25-30% openings in the façade. These structures are constructed on ground type C following a seismic excitation of

0.3g. The range for each case is established by considering the highest and lowest values of correction factors that correspond to different structural materials. It is evident that most structures subjected to these conditions do not experience significant damage, except those made of adobe.

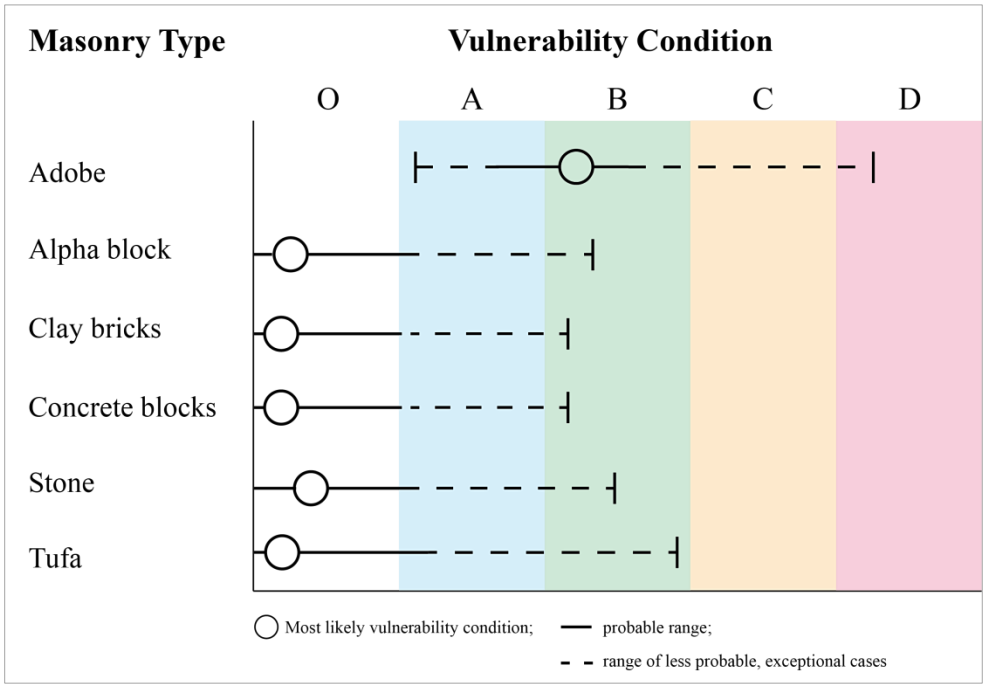

Figure 4. Vulnerability table

7. Conclusion

This research aims to introduce the PRISM form, a streamlined pre-seismic survey document designed exclusively for masonry structures. This form serves both experienced engineers and newcomers in the field. While many existing pre- and post-seismic survey forms rely on empirical guidelines, the PRISM form is established through numerical and parametric analysis. Most of the information required to complete the form aligns with other survey documents. This includes inputs such as the primary structural material, number of floors, and ground characteristics, including acceleration. These aspects, along with others, collectively influence the capacity of a structure to withstand lateral forces caused by dynamic events like earthquakes and wind. The essential contribution here is quantifying this influence's degree, often represented as a percentage.

For instance, the impact of openings on the façade of a masonry structure is commonly understood—more openings usually correspond to reduced stiffness. With the PRISM form, a surveyor can readily grasp, for example, that in a tufa structure, the presence of wooden casings for openings contributes to a 3% increase in stiffness. In comparison, the utilization of aluminum casings results in a 14% increase. The importance of this research transcends the boundaries of the surveying realm. Consider a junior engineer or architect who, by consulting the vulnerability table, gains insights into why adobe structures within the city exhibit extensive damage. In contrast, buildings and historical monuments constructed from tufa stone remain relatively unscathed.

Notably, Eurocode 6 does not account for masonry structures made of adobe or tufa. However, since all masonry materials exhibit brittleness and the plastic region of stress-strain curves is not considered, understanding stiffness differences, mainly through the displacement results presented in Table 4, between adobe blocks and clay bricks (which Eurocode 6 covers), empowers engineers to make informed decisions about retrofitting or mitigation strategies.

In summary, the quantitative outcomes of this study, combined with the utility of the PRISM form as a tool for pre-seismic surveys, offer significant benefits. These extend to developing risk assessment maps, informed decision-making, and aiding design engineers and students in their endeavors.

8. Declarations

8.1. Author Contributions

Conceptualization, G.X.; methodology, G.X.; software, G.X.; validation, D.P., G.Z., and P.C.; formal analysis, G.X.; investigation, G.X.; resources, G.X.; data curation, G.X.; writing—original draft preparation, G.X.; writing—review and editing, D.P., P.C., and G.Z.; visualization, G.X.; supervision, P.C.; project administration, P.C.; funding acquisition, P.C. All authors have read and agreed to the published version of the manuscript.

8.2. Data Availability Statement

The data presented in this study are available in the article.

8.3. Funding

This research work was supported by the ISTOS project. This project has received funding from the European Union's Horizon 2020 research and innovation program (WIDESPREAD-TWINNING) under grant agreement No. 952300.

8.4. Conflicts of Interest

The authors declare no conflict of interest.

9. References

[1] Xekalakis, G., & Christou, P. (2023). Tracing the Historical Development of Architecture in Cyprus and its Resilience to Seismic Hazards. International Journal of Architectural Engineering Technology, 10, 1–15. doi:10.15377/2409-9821.2023.10.1.

[2] Puncello, I., & Caprili, S. (2023). Seismic Assessment of Historical Masonry Buildings at Different Scale Levels: A Review. Applied Sciences (Switzerland), 13(3), 1941. doi:10.3390/app13031941.

[3] Lovett, R.A. (2011). Europe Starting to Dive Under Africa? National Geographic Society, Washington, United States. Available online: https://www.nationalgeographic.com/science/article/110419-europe-africa-mediterranean-earthquake-risk-increasing-earth-science (accessed on October 2023).

[4] Bernardo, V., Sousa, R., Candeias, P., Costa, A., & Campos Costa, A. (2022). Historic Appraisal Review and Geometric Characterization of Old Masonry Buildings in Lisbon for Seismic Risk Assessment. International Journal of Architectural Heritage, 16(12), 1921–1941. doi:10.1080/15583058.2021.1918287.

[5] Zeng, B., & Li, Y. (2023). Towards Performance-Based Design of Masonry Buildings: Literature Review. Buildings, 13(6), 1534–1534. doi:10.3390/buildings13061534.

[6] Dong, Z. Q., Li, G., Song, B., Lu, G. H., & Li, H. N. (2022). Failure risk assessment method of masonry structures under earthquakes and flood scouring. Mechanics of Advanced Materials and Structures, 29(21), 3055–3066. doi:10.1080/15376494.2021.1884322.

[7] Zuccaro, G., Dolce, M., Perelli, F. L., De Gregorio, D., & Speranza, E. (2023). CARTIS: a method for the typological-structural characterization of Italian ordinary buildings in urban areas. Frontiers in Built Environment, 9. doi:10.3389/fbuil.2023.1129176.

[8] Funari, M. F., Spadea, S., Lonetti, P., Fabbrocino, F., & Luciano, R. (2020). Visual programming for structural assessment of out-of-plane mechanisms in historic masonry structures. Journal of Building Engineering, 31, 101425–101425. doi:10.1016/j.jobe.2020.101425.

[9] Stepinac, M., & Gašparović, M. (2020). A review of emerging technologies for an assessment of safety and seismic vulnerability and damage detection of existing masonry structures. Applied Sciences (Switzerland), 10(15), 5060. doi:10.3390/app10155060.

[10] Sanrı Karapınar, I., Özbay, A. E. Ö., & Ünen, H. C. (2021). GIS-Based Assessment of Seismic Vulnerability Information of Old Masonry Buildings Using a Mobile Data Validation System. Journal of Performance of Constructed Facilities, 35(3), 04021009. doi:10.1061/(asce)cf.1943-5509.0001574.

[11] Brando, G., Cianchino, G., Rapone, D., Spacone, E., & Biondi, S. (2021). A CARTIS-based method for the rapid seismic vulnerability assessment of minor Italian historical centres. International Journal of Disaster Risk Reduction, 63, 102478. doi:10.1016/j.ijdrr.2021.102478.

[12] Valkonen, A., & Glisic, B. (2022). Evaluation tool for assessing the influence of structural health monitoring on decision-maker risk preferences. Structural Health Monitoring, 21(1), 90–99. doi:10.1177/1475921721992016.

[13] Menteşe, E. Y., Cremen, G., Gentile, R., Galasso, C., Filippi, E. M., & McCloskey, J. (2023). Future exposure modelling for risk-informed decision making in urban planning. International Journal of Disaster Risk Reduction, 90, 103651. doi:10.1016/j.ijdrr.2023.103651.

[14] CSI. (2023). SAP2000: Computers and Structures, Inc. Available online: https://www.csiamerica.com/products/sap2000 (accessed on June 2023).

[15] Foti, D. (2013). On the numerical and experimental strengthening assessment of tufa masonry with FRP. Mechanics of Advanced Materials and Structures, 20(2), 163–175. doi:10.1080/15376494.2012.743634.

[16] Mollaei, S., Babaei Ghazijahani, R., Noroozinejad Farsangi, E., & Jahani, D. (2022). Investigation of Behavior of Masonry Walls Constructed with Autoclaved Aerated Concrete Blocks under Blast Loading. Applied Sciences, 12(17), 8725. doi:10.3390/app12178725.

[17] Christou, P., & Xekalakis, G. (2022). The Contribution of Wooden Ring Beams to the Response of the Adobe Structures. Proceedings of International Structural Engineering and Construction, 9(1), AAE-14-1-5. doi:10.14455/isec.2022.9(1).aae-14.

[18] Fudge, C., Fouad, F., & Klingner, R. (2019). Autoclaved aerated concrete. In Developments in the Formulation and Reinforcement of Concrete. Woodhead Publishing Series in Civil and Structural Engineering, 345-363. doi:10.1016/B978-0-08-102616-8.00015-0.

[19] Nichols, J.M., & Totoev, Y.Z. (2003). Experimental determination of the dynamic Modulus of Elasticity of masonry units. Proceedings of the 11th International Brick and Block Masonry Conference, Shanghai, China.

[20] Heap, M. J., Baud, P., Meredith, P. G., Vinciguerra, S., & Reuschlé, T. (2014). The permeability and elastic moduli of tuff from Campi Flegrei, Italy: Implications for ground deformation modelling. Solid Earth, 5(1), 25–44. doi:10.5194/se-5-25-2014.

[21] project, I. S. T. O. S. (n.d.). Home. http://istoscenter.eu/.

[22] Sfaksi, O. H., Bouheraoua, A., Aider, H. A., & Mechiche, M. O. (2022). Seismic Behavior of Reinforced Masonry Structure: Relation between the Behavior Factor and the Ductility. Civil Engineering Journal, 8(10), 2205-2219. doi:10.28991/CEJ-2022-08-10-012.

[23] The Engineering ToolBox. (2019). Poisson's Ratio. Available online: https://www.engineeringtoolbox.com/poissons-ratio-d_1224.html (accessed on June 2023).

[24] Thyssenkrupp. (2018). Density of Aluminium. Thyssenkrupp Materials, Cox's Lane, United Kingdom. Available online: https://www.thyssenkrupp-materials.co.uk/density-of-aluminium.html (accessed on October 2023).

[25] Metaweb. (2023). Overview of materials for PVC, Extruded. Material Properties Data, Metaweb. Available online: https://matweb.com/search/datasheet_print.aspx?matguid=bb6e739c553d4a34b199f0185e92f6f7 (accessed on May 2023).

[26] Annecchiarico, M., Portioli, F., & Landolfo, R. (2010). Micro and macro finite element modeling of brick masonry panels subject to lateral loadings. Urban Habitat Constructions under Catastrophic Events (Proceedings), STAMPA, 315-320.

[27] CSI. (2023). Shell - Technical Knowledge Base - Computers and Structures, Inc. - Technical Knowledge Base. Computers and Structures, Inc, Walnut Creek, United States. Available online: https://wiki.csiamerica.com/display/kb/Shell (accessed on October 2023).

[28] European Commission. (2014). Mapping Europe's earthquake risk. European Commission, Brussels, Belgium. Available online: https://ec.europa.eu/research-and-innovation/en/horizon-magazine/mapping-europes-earthquake-risk (accessed on October 2023).

[29] EN 1998-1. (2004). Design of structures for earthquake resistance Part 1: General rules, seismic actions and rules for buildings. European Committee for Standardization, Brussels, Belgium.

[30] Tomaževič, M., Bosiljkov, V., & Weiss, P. (2004). Structural behaviour factor for masonry structures. 13th world conference on earthquake engineering, 1-6 August, 2004, Vancouver, Canada.

[31] Misir, I. S., & Yucel, G. (2023). Numerical Model Calibration and a Parametric Study Based on the Out-Of-Plane Drift Capacity of Stone Masonry Walls. Buildings, 13(2), 437. doi:10.3390/buildings13020437.

[32] Vlachakis, G., Cervera, M., Barbat, G. B., & Saloustros, S. (2019). Out-of-plane seismic response and failure mechanism of masonry structures using finite elements with enhanced strain accuracy. Engineering Failure Analysis, 97, 534–555. doi:10.1016/j.engfailanal.2019.01.017.

[33] Zavala, C., Diaz, M., Flores, E., & Cardenas, L. (2019). Damage limit states for confined masonry walls based on experimental test. Tecnia, 29(2). doi:10.21754/tecnia.v29i2.715.

[34] Shabani, A., Plevris, V., & Kioumarsi, M. (2021). A comparative study on the initial in-plane stiffness of masonry walls with openings. In Proceedings of the World Conference on Earthquake Engineering, 17WCEE, 27 September-2 October, Sendai, Japan.

[35] Zuccaro, G., & Cacace, F. (2015). Seismic vulnerability assessment based on typological characteristics. The first level procedure "SAVE." Soil Dynamics and Earthquake Engineering, 69, 262–269. doi:10.1016/j.soildyn.2014.11.003.

[36] GFZ. (2023). Macroseismic Intensity Scale: Classifications used in the European Macroseismic Scale (EMS). Available online: https://media.gfz-potsdam.de/gfz/sec26/resources/documents/PDF/EMS-98_core_part_English.pdf (accessed on May 2023).